

ASSESSMENT OF ENGINE-OUT ATMOSPHERIC EMISSIONS FROM COCONUT-OIL-DERIVED BIOJET FUEL

Shinichiro Ogawa[1], Takuto Hongo[1], Yasuaki Maeda[2], H. P. Uyen Nguyen[2] & Koichi Mori[1]

[1]Department of Aerospace and Marine-System Engineering, Osaka Metropolitan University
[2]Department of Environmental Sciences, Osaka Metropolitan University

Abstract

This study evaluated the engine performance and atmospheric environmental impact of coconut-oil-derived biofuel blends in a small turbojet engine. Biofuel was produced from non-standard coconut oil using a low-energy co-solvent method. The resulting fuel was primarily composed of ethyl octanoate and ethyl decanoate, with a purity of 97.66%. Combustion experiments were conducted using a small turbojet engine with biofuel blend ratios of 10–50%, and the combustion efficiency, specific fuel consumption, and exhaust emission index of CO, CO_2, and NO were analyzed. The results showed that B20 and B30 maintained combustion efficiencies comparable to those of conventional jet fuel, whereas B30 exhibited the lowest specific fuel consumption over the tested rotational speed range. The emission indices of CO_2 and NO generally decreased with increasing biofuel blend ratio, particularly under high rotational speed conditions, whereas CO emissions showed non-monotonic behavior depending on the blend ratio and operating conditions. The LTO-cycle-based emission analysis indicated that the taxi/idle phase dominated the total CO_2 and NO emissions because of its long operating duration. In addition, atmospheric dispersion analysis using a Gaussian plume model revealed that NO concentrations decreased substantially with increasing biofuel content; at 100,000 rpm, the predicted NO concentration 10 m downstream decreased by approximately 36% for B50 compared with that of the conventional fuel. These results demonstrate that coconut oil-derived biofuel blending can reduce NO emissions and modify near-field atmospheric concentration distributions, although further optimization of fuel atomization and combustion characteristics is required to suppress CO emissions at high blend ratios.

Keywords: Boifuel, Coconut oil, Small turbojet engine, Combustion characteristics, Exhaust gas

1. Introduction

Biofuels have attracted considerable attention as promising substitutes for petroleum-derived aviation fuels owing to their potential to reduce life-cycle CO_2 emissions and thereby contribute to the decarbonization of the aviation sector. However, their widespread implementation is constrained by limited feedstock availability, high production costs, and energy-intensive conversion processes[1, 2]. In Japan, aviation biofuels are produced primarily from waste cooking oil, the supply of which is limited and costly, underscoring the need to identify alternative, regionally available feedstocks.

This study focused on non-standard coconuts discarded in Southeast Asia as a potential feedstock for aviation biofuel production. During coconut cultivation and processing, a certain proportion of coconuts are classified as non-standard owing to insufficient size, premature sprouting, cracking, or spoilage, rendering them unsuitable for edible applications[3]. Although such non-standard coconuts are considered low-value or unused by-products, they retain oil components that can be converted into liquid biofuels. Under the CORSIA methodology, non-standard coconuts have been recognized as a potential sustainable aviation fuel feedstock, with a default life-cycle emission value of 26.9 gCO_2e/MJ[3]. Because these coconuts are treated as agricultural by-products, the contribution of

direct land-use change to the life-cycle assessment can be reduced or excluded. Accordingly, the utilization of non-standard coconut oil is expected to enable both effective valorization of an underused waste resource and a substantial reduction in life cycle CO_2 emissions relative to petroleum-derived jet fuel. Coconut oil contains a high proportion of medium-chain fatty acids, and its carbon-number distribution closely resembles that of conventional jet fuel components[4, 5]. Coconut-oil-derived fatty acid esters are therefore considered promising candidates for liquid aviation fuel applications, particularly as blending components with conventional jet fuel.

Although several biofuel production pathways have been certified under ASTM D7566 [6], many of these processes require high-temperature, high-pressure, and hydrogen-consuming conditions. In contrast, the present study employs a low-energy co-solvent transesterification method using ethanol and acetone [7]. This method enables high biofuel yields under comparatively mild conditions, namely approximately 50 °C and atmospheric pressure, and is therefore expected to reduce the energy consumption associated with fuel production relative to conventional catalytic hydrogenation routes [8, 9]. Previous studies have investigated the combustion and emission characteristics of HEFA, FAME, and other biofuel blends in diesel engines and gas turbine systems [10, 11, 12, 13]. However, the combustion performance, exhaust emission characteristics, LTO-cycle emissions, and atmospheric environmental impact of coconut-oil-derived biofuel blends in small gas turbine engines remain insufficiently understood.

This study evaluated the applicability and atmospheric environmental impact of coconut-oil-derived biofuel blends produced via a low-energy co-solvent method. Combustion experiments were conducted using a small-scale jet engine with biofuel blend ratios ranging from 10% to 50% in volume. The combustion efficiency, specific fuel consumption, and major exhaust emission species, including HC, CO, CO_2, and NO, were analyzed. In addition, the LTO cycle emissions and atmospheric concentration distributions were estimated based on the experimentally measured exhaust gas compositions. Through this integrated evaluation, the potential of coconut-oil-derived biofuel blending to mitigate the environmental burden of small gas-turbine engines was assessed.

2. Biofuel

In this study, biofuel was synthesized from coconut oil using a low-energy co-solvent method[7, 14, 15] with ethanol and acetone. Compared with conventional alkaline transesterification and ultrasound-assisted processes, this method enables rapid and high-efficiency conversion under low-temperature and atmospheric-pressure conditions while suppressing soap formation.

The production process involved mixing a coconut oil–acetone solution with an ethanol–KOH solution in a stirred reactor. When the acetone content was at least 10 wt% and the catalyst concentration was 0.2–0.8 wt%, transesterification proceeded rapidly, achieving conversion rates above 80% within 2–10 min even at 10–20 °C. After the reaction, spontaneous phase separation occurred, allowing the glycerin-rich phase to separate easily from the ester-rich phase. Residual ethanol and acetone were subsequently removed by distillation and reused.

After washing and dehydration, a high-quality coconut-oil-derived biofuel with a purity of 97.66% was produced. HPLC(High Performance Liquid Chromatography) analysis showed that the product mainly consisted of ethyl octanoate and ethyl decanoate, with mass fractions of 41.2 wt% and 56.5 wt%, respectively. The remaining 2.3 wt% consisted of residual glycerides and free fatty acids. These results indicate that the produced biofuel was primarily composed of medium-chain fatty acid ethyl esters, whose carbon-number range is suitable for use as a blending component for jet fuel.

The produced biofuel was blended with conventional jet fuel (Jet A-1) at volumetric or mass blending ratios of 10–50%. Neat conventional jet fuel was denoted as J100, whereas the biofuel blends were denoted as B10, B20, B30, B40, and B50, corresponding to biofuel blending ratios of 10, 20, 30, 40, and 50%, respectively.

3. Experimental setup

In this study, the effects of biofuel blending on engine performance and exhaust emission characteristics were evaluated using small turbojet engine. The experimental apparatus comprised a small turbojet engine, fuel supply system, thrust measurement system, temperature and pressure mea-

surement system, rotational speed measurement system, and exhaust gas analyzer. A schematic of the experimental apparatus is shown in Fig. 1.

A small turbojet engine (J-850 engine, Sophia Precision)[16, 17, 18] was used as the test engine. This engine is a single-spool gas turbine engine that consists of a compressor, combustor, turbine, and exhaust nozzle. Ambient air is drawn in and compressed by the compressor, mixed with fuel, and combusted in the combustor to generate a high-temperature and high-pressure gas. The combustion gas subsequently passes through the turbine, delivering the work required to drive the compressor before being expelled at high velocity through the exhaust nozzle to produce thrust. In the present study, the engine rotational speed was controlled under prescribed conditions, and the thrust, fuel consumption, combustion efficiency, and exhaust gas composition were measured for each fuel condition.

The fuel supply system consisted of a fuel tank, fuel lines, a fuel pump, and a fuel flow meter. The fuel was supplied from the fuel tank by a pump, and the fuel flow rate was measured before it was introduced into the engine combustor. In this study, conventional fuel and biofuel-blended fuels were investigated, and the effects of fuel property variations on combustion and exhaust emission characteristics were evaluated by varying the biofuel blending ratios.

Thrust was measured using a load cell installed on the test stand to which the engine was attached. The axial thrust generated during engine operation was detected using a load cell, and the resulting signal was recorded using a data acquisition system. Temperature measurements were performed using thermocouples installed at the compressor inlet and outlet, turbine inlet and outlet, and exhaust sections. Pressure measurements were conducted using pressure sensors to acquire the inlet and exit pressures of the compressor.

The acquired data were used to calculate the specific fuel consumption and combustion efficiencies. The combustion efficiency (η_b), was evaluated as the ratio of the enthalpy rise across the combustor to the chemical energy supplied by the fuel, as expressed by

$$\eta_b = \frac{(1+f)c_p(T_3 - T_2)}{f \cdot LHV} \tag{1}$$

where f is the fuel–air ratio, c_p is the specific heat at constant pressure of the working fluid [J/(kg·K)], T_2 is the combustor inlet temperature [K], T_3 is the combustor exit temperature [K], and LHV is the lower heating value of the fuel [J/kg]. The specific fuel consumption (SFC) was calculated by dividing the fuel mass flow rate ($\dot{m}_f$) by the thrust (F) as follows:

$$SFC = \frac{\dot{m}_f}{F} \tag{2}$$

where SFC is the specific fuel consumption [kg/(N·s)], $\dot{m}_f$ is the fuel mass flow rate [kg/s], and F is the thrust [N].

The exhaust gas composition was measured using an exhaust gas analyzer, MEXA-584L (HORIBA). The exhaust gas was sampled using a probe installed downstream of the engine exhaust outlet and introduced into the analyzer. The measured species included CO, CO_2, and NO, and the exhaust gas concentrations were obtained for each operating condition. Based on the measured exhaust gas concentrations and fuel flow rates, the emission index of each species was calculated. The emission index was defined as the mass of each species emitted per unit mass of fuel consumed and was used to compare the emission characteristics under different fuel conditions.

In the experiments, the engine rotational speed was increased to the prescribed value after the startup, and measurements were performed after the operating conditions became stable. Under each fuel condition, the thrust, fuel flow rate, temperature, pressure, and exhaust gas composition were acquired simultaneously under identical rotational speed conditions. This procedure enabled a systematic evaluation of the effects of the biofuel blending ratio on the engine performance and exhaust emission characteristics.

4. Results and Disucssion

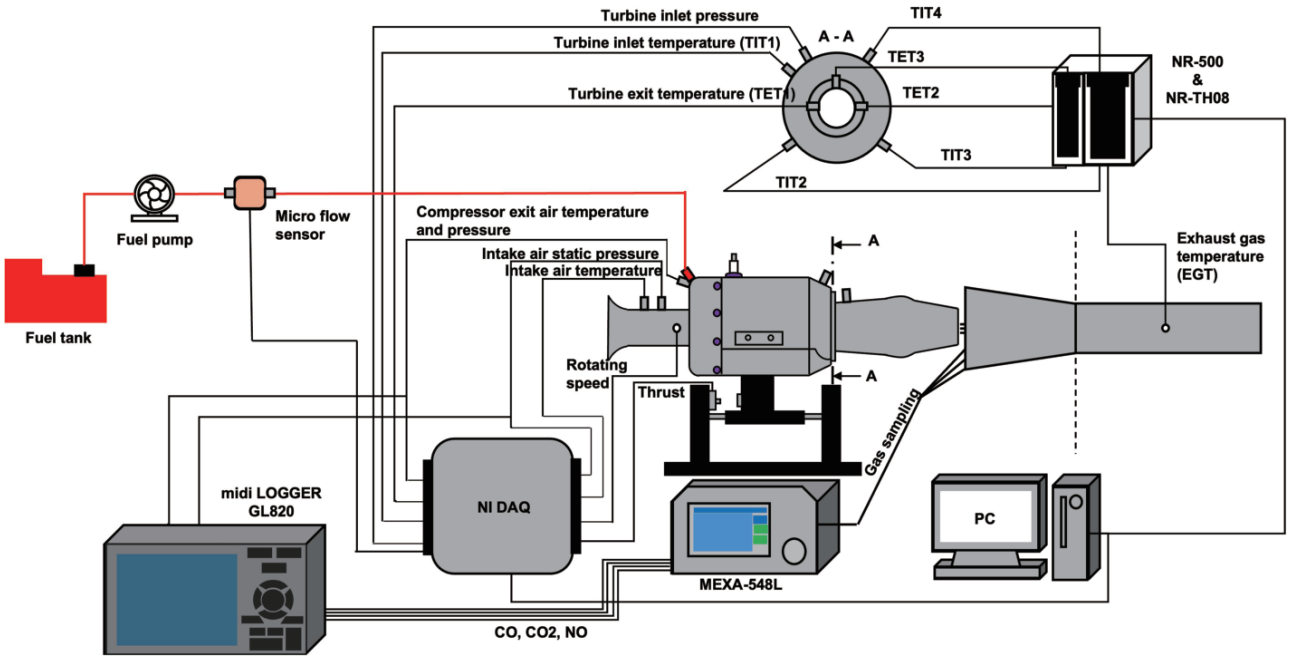


Figure 1 – Schematic diagram of the experimental setup for the small turbojet engine.

4.1 Combustion Efficiency and Fuel Specific Consumption

Figure 2 shows the combustion efficiency for biofuel blend ratios of 0–50%. Overall, the combustion efficiency varied depending on both the fuel conditions and engine rotational speed. For J100, the combustion efficiency increased with increasing rotational speed and reached its maximum value at 100,000 rpm. This trend is considered to be attributable to enhanced fuel atomization, increased air flow rate, and improved fuel–air mixing under high rotational speed conditions, which promoted more complete combustion.

In contrast, the combustion efficiencies of the biofuel-blended fuels exhibited different trends depending on the blend ratio. B20 and B30 showed relatively high combustion efficiencies over the entire rotational speed range, with average values of approximately 89.9% and 89.3%, respectively. These values were close to the average value of J100, approximately 91.1%, indicating that a combustion performance comparable to that of conventional fuel can be maintained even when 20–30% biofuel is blended. In particular, B20 showed a high combustion efficiency of approximately 89–91% over the rotational speed range of 80,000–95,000 rpm, demonstrating stable combustion characteristics with respect to changes in engine rotational speed.

In contrast, B10 and B40 exhibited reductions in combustion efficiency under certain rotational speed conditions. For B10, the combustion efficiency was low at 80,000 and 90,000rpm, and the average value remained at approximately 83.3%. Similarly, B40 decreased to approximately 80% at 85,000 and 90,000rpm. These results suggest that at low or specific blend ratios, changes in fuel properties may affect the spray, evaporation, and mixing processes, thereby reducing the combustion completeness. In contrast, B50 exhibited a high combustion efficiency of 93.9% at 90,000 rpm, although its values at other rotational speeds were slightly lower than those of J100. Therefore, the combustion efficiency did not change monotonically with increasing biofuel blend ratio, suggesting that the combination of fuel properties and engine operating conditions at each blend ratio strongly affected the combustion efficiency.

Figure 3 shows the specific fuel consumption for different biofuel blend ratios in the present study. Under all fuel conditions, the SFC decreased with increasing rotational speed. This is because, under high rotational speed conditions, the increase in fuel consumption becomes relatively small compared with the increase in thrust, resulting in improved engine operating efficiency. In particular, at 100,000 rpm, the SFC reached its minimum value for all fuel conditions, indicating improved fuel utilization efficiency in the high rotational speed range.

Regarding the effect of fuel condition, B30 exhibited the lowest SFC across the entire rotational speed

range. The average SFC of B30 was approximately (6.41 $\times 10^{-5}$) kg/Ns, which was approximately 12% lower than the average value of J100, (7.30 $\times 10^{-5}$) kg/Ns. B10 and B20 also exhibited lower SFC values than J100, with average reductions of approximately 9.6% and 7.4%, respectively. These results indicate that the engine can be operated with reduced fuel consumption when an appropriate biofuel blend ratio is selected.

Although the SFC values of B40 and B50 were lower than those of J100, they were higher than those of B30. In particular, B50 exhibited high combustion efficiency under certain conditions, but its SFC reduction effect was less pronounced than that of B30. This may be because increasing the biofuel blend ratio changes the lower heating value, viscosity, density, and evaporation characteristics of the fuel, thereby increasing the amount of fuel required to obtain the same thrust level. Therefore, under high blend ratio conditions, the optimal blend ratio should be evaluated not only in terms of combustion efficiency but also from the viewpoint of fuel consumption.

These results indicate that the combustion performance of biofuel-blended fuels strongly depends on the blend ratio and should be evaluated in terms of both the combustion efficiency and SFC. B20 and B30 maintained high combustion efficiencies close to that of J100 while reducing SFC. In particular, B30 exhibited the lowest SFC over the entire rotational speed range, indicating that it is an effective blend ratio for improving the fuel economy. In contrast, B10 and B40 showed reduced combustion efficiency under certain conditions, whereas B50 exhibited a relatively high combustion efficiency but only a limited improvement in SFC. Therefore, under the present experimental conditions, a biofuel blend ratio of approximately 20–30% is considered to provide a favorable balance between combustion stability and fuel consumption.

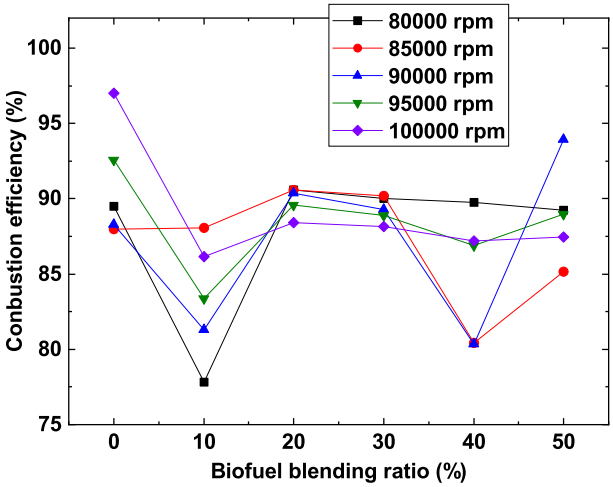


Figure 2 – Combustion efficiency as a function of engine rotational speed for different biofuel blend ratios.

4.2 Exhaust Gas

Figure 4 presents the relationship between the biofuel blend ratio and emission index[19, 20] at engine rotational speeds of 80,000, 90,000, and 100,000 rpm. The species evaluated were CO, CO_2, and NO, organized as EICO, EICO2, and EINO, respectively. Overall, the emission indices of CO_2 and NO exhibited a decreasing trend with an increasing biofuel blend ratio. In contrast, the emission index of CO did not vary monotonically with either the blend ratio or rotational speed, confirming that it is strongly governed by differences in combustion conditions.

At 80,000 rpm, EICO2 initially increased at a blend ratio of 10%, then decreased with further increases in the blend ratio. In particular, B50 exhibited a marked reduction in EICO2 relative to J100, confirming the CO_2 emission reduction associated with biofuel blending. EINO similarly reached its maximum at B10, followed by a decreasing trend from B20 onward, and reached its minimum at B50. These findings suggest that under high blend ratio conditions, the reduction in the carbon content of the fuel and changes in the combustion temperature may have suppressed the formation of both CO_2 and NO. Meanwhile, EICO was elevated at B10 and B20, decreased in the vicinity of B40, and

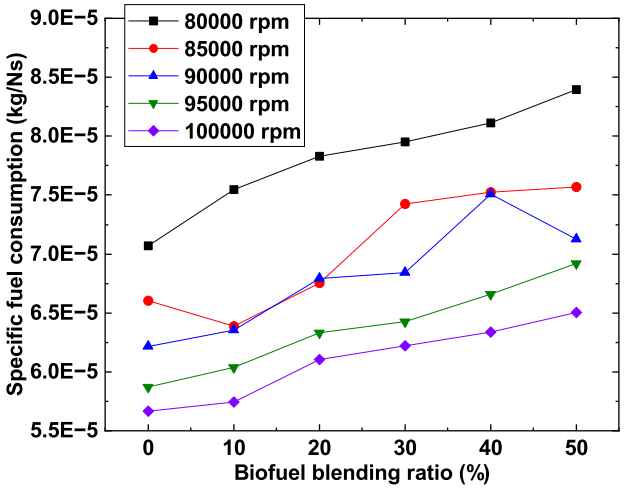


Figure 3 – Specific fuel consumption (SFC) as a function of engine rotational speed for different biofuel blend ratios.

showed a slight increase at B50. Because CO serves as an indicator of incomplete combustion, it is considered that under relatively low rotational speed conditions, such as 80,000 rpm, changes in fuel spray, evaporation, and air-mixing behavior influenced CO production.

At 90,000 rpm, EICO2 and EINO reached their maximum values at B10 and then generally decreased with increasing blend ratio. In particular, B40 and B50 yielded lower EICO2 and EINO than J100, demonstrating that high-blend ratio biofuels are effective in reducing CO_2 and NO emissions. Meanwhile, EICO increased at B10, decreased at B30, and increased again at B40. These results indicate that while CO_2 and NO reduction effects are achievable, combustion completeness varies with the blend ratio. That is, biofuel blending alters the oxygen content and combustion temperature of the fuel, thereby suppressing NO formation, whereas changes in the spray and evaporation characteristics may have induced localized incomplete combustion.

At 100,000 rpm, EICO2 exhibited an elevated value at B10, then decreased continuously from B20 onward, reaching its minimum value at B50. EINO similarly reached its maximum at B10 and subsequently decreased with increasing blend ratio, attaining its lowest value at B50. Under high rotational speed conditions, the increased air mass flow rate and fuel spray momentum enhance fuel–air mixing, thereby improving the combustion conditions. As a result, stable combustion was maintained even at high blend ratios, and the reduction effects on CO_2 and NO were clearly observed. In contrast, EICO increased for B10 and B20 relative to J100 but decreased from B30 onward, reaching its minimum at B40. These findings suggest that at 100,000 rpm, blend ratios in the range of B30–B50 have the potential to suppress CO emissions while simultaneously reducing CO_2 and NO.

With regard to the effect of engine rotational speed, the decreasing trends in EICO2 and EINO with respect to the biofuel blend ratio became more pronounced as the rotational speed increased. In particular, at 100,000 rpm, EICO2 and EINO decreased continuously from B20 onward, indicating that the effects of biofuel blending were most prominently expressed under high rotational speed conditions. This is attributed to the fact that higher rotational speeds promote finer atomization of the fuel spray and enhanced mixing with air, thereby allowing the combustion characteristics of the biofuel to be utilized more effectively. Under low rotational speed conditions, on the other hand, the influence of differences in fuel viscosity, density, and evaporation characteristics on the combustion field becomes relatively more significant, potentially contributing to increases in EICO and fluctuations in EINO.

In summary, biofuel blending effectively reduced the emission indices of CO_2 and NO, with the effect being particularly pronounced under high blend ratio conditions of B40 and B50. Furthermore, this reduction effect was more clearly observed under high rotational speed conditions. In contrast, CO emissions did not vary monotonically with the blend ratio, and increases were observed under certain conditions. Therefore, when evaluating the environmental benefits of blended biofuels, a comprehensive assessment is required that encompasses not only the reduction of CO_2 and NO but also the

potential increase in CO emissions. Under the experimental conditions of this study, the high blend ratio conditions of B40–B50 yielded the greatest reductions in CO_2 and NO, and CO emissions were also maintained at relatively low levels at 100,000 rpm, suggesting the effectiveness of high-blend-ratio biofuels in the high rotational speed regime.

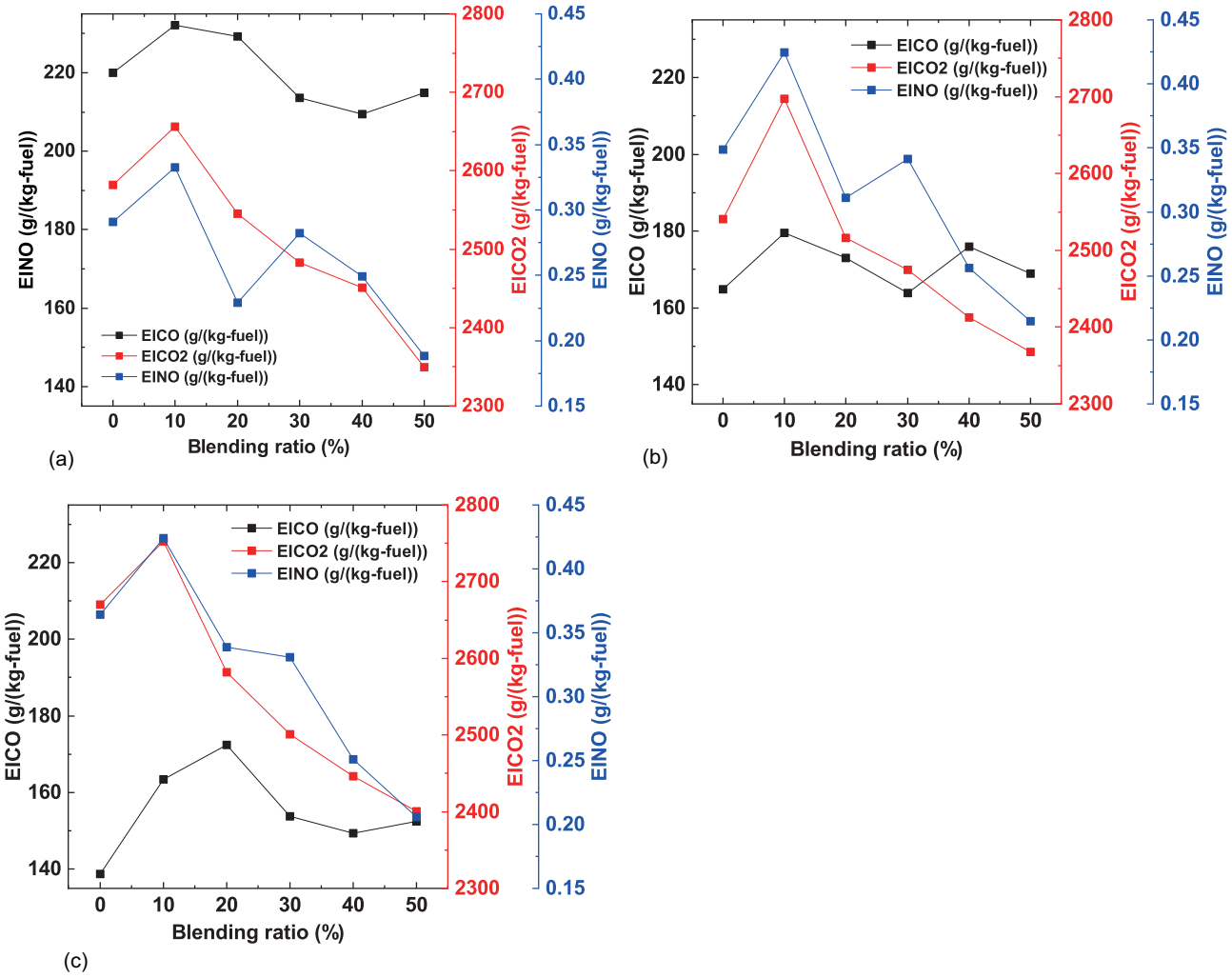


Figure 4 – Emission index of CO, CO_2, and NO (EICO, EICO2, EINO) as functions of biofuel blend ratio at engie rotational speeds of (a) 80,000, (b) 90,000, and (c) 100,000 rpm.

4.3 LTO Cycle

Next, the environmental impact of aircraft emissions during flight operations was evaluated using the Landing and Takeoff (LTO) cycle[21, 22]. As shown in Fig. 5, the LTO cycle is a standardized assessment cycle covering operational conditions below an altitude of 3,000 ft, comprising the approach, taxi/idle, takeoff, and climb-out phases. Because pollutants emitted within this altitude range directly affect the air quality in the vicinity of airports, the LTO cycle is widely employed to estimate aircraft-derived atmospheric pollutant emissions around airport environments. In this chapter, the focus is placed on CO_2 and NO emissions.

In the LTO cycle, the cycle time and rated thrust setting for each operational phase are prescribed by the ICAO, and the corresponding conditions are summarized in Table 1. The emissions during the LTO cycle were calculated as the product of the fuel flow rate, emission index per unit fuel consumption, and cycle time for each phase. Accordingly, the total emissions over the entire LTO cycle are expressed as follows.

$$E_{\mathrm{LTO}} = \sum_i \dot{m}_{f,i}, EI_i, t_i \tag{3}$$

where E_{LTO} denotes the total emissions over the entire LTO cycle [kg/LTO], $\dot{m}_{f,i}$ is the fuel flow rate at

each operational phase i [kg/s], EI_i is the emission index per unit fuel consumption [kg/kg-fuel], and t_i is the duration of each phase [s].

Figure 6 shows the CO_2 emissions during the LTO cycle for biofuel blend ratios of 0–50%. Under all fuel conditions, the taxi/idle phase contributed most significantly to the total CO_2 emissions. This is attributable to the fact that, although the thrust setting during taxi/idle is as low as 7%, the operating duration of 1,560 s is significantly longer than that of the other phases. In contrast, although the take off and climb-out phases operate at higher thrust setting, their durations are relatively short at 42 s and 132 s, respectively, resulting in comparatively smaller contributions to the overall LTO cycle emissions.

Regarding the differences among the fuel conditions, CO_2 emissions ere reduced for B10 and B20 relative to J100. Meanwhile, B30 and B40 exhibited values comparable to those of J100, and B50 showed a tendency toward a renewed reduction. These results indicate that CO_2 emissions do not vary monotonically with increasing biofuel blend ratio, suggesting that the combined effects of fuel consumption, fuel composition, and differences in combustion behavior in each operational phase contribute in a complex manner.

Figure 6 shows the NO emissions during the LTO cycle. As with CO_2, the taxi/idle phase accounted for the largest share of NO emissions. In particular, because taxi/idle occupies the majority of the total LTO cycle duration, it exerts a substantial influence on the total emissions even under low-thrust conditions. Furthermore, NO emissions varied considerably with fuel conditions; B20 and B50 exhibited a clear reduction compared to J100. Notably, B20 yielded the lowest total NO emissions over the entire LTO cycle, demonstrating a pronounced NO reduction effect, which was attributable to biofuel blending. In contrast, B30 and B40 showed values close to those of J100, indicating that the NO reduction effect did not vary monotonically with the blend ratio.

In summary, the LTO cycle-based assessment revealed that emissions affecting air quality in the vicinity of airports are strongly dependent on the taxi/idle phase. Furthermore, although biofuel blending demonstrates a certain degree of effectiveness in reducing both CO_2 and NO emissions, the magnitude of this effect is not necessarily monotonic with respect to the blend ratio, suggesting a dependence on changes in fuel properties and combustion characteristics. In particular, B20 and B50 were confirmed to reduce NO emissions, indicating their potential as effective fuel conditions for mitigating environmental burdens in the LTO cycle.

Table 1 – Thrust and time at each phase of the LTO cycle.

LTO cycle	Thrust power, %	Time, s
Take off (T/O)	100	42
Climb out (C/O)	85	132
Approach (App)	30	240
Taxi/Idle (Idle)	7	1560

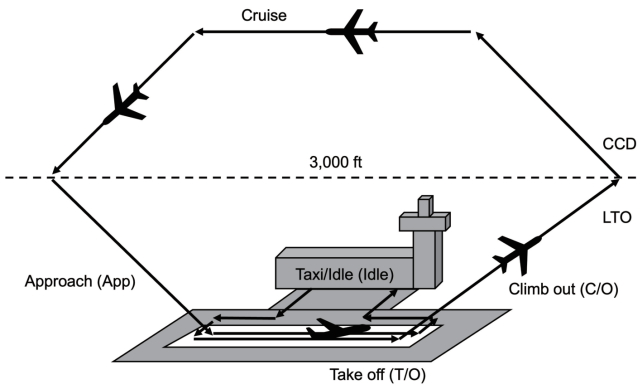


Figure 5 – Schematic of the landing and take-off (LTO) cycle, showing the operational phases below an altitude of 3,000 ft.

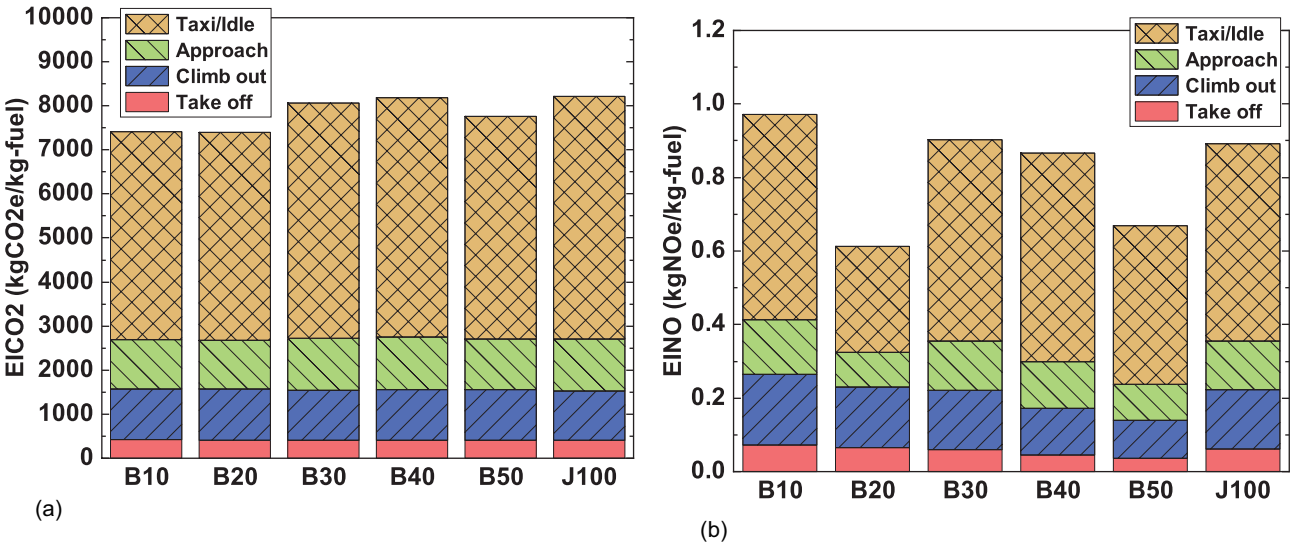


Figure 6 – CO_2 and NO emissions for each phase of the LTO cycle at different biofuel blend ratios, (a) CO_2, and (b) NO.

4.4 Atmospheric Concentration Distribution of Exhaust Specie

To evaluate the environmental impact of exhaust emissions from a small gas turbine engine, an atmospheric dispersion analysis was performed using a Gaussian plume model[23] based on experimentally measured exhaust gas compositions. The concentrations of CO, HC, NO, and CO_2 were measured using an exhaust gas analyzer, and the exhaust gas temperature (T_4) and exhaust velocity (v_5) were obtained from engine performance measurements. The exhaust gas density (ρ_e) was estimated using the ideal gas law,

$$\rho_e = \frac{P_e}{RT_4} \tag{4}$$

where P_e is the exhaust pressure, and R is the specific gas constant of air. The exhaust mass flow rate ($\dot{m}_e$) was subsequently calculated as

$$\dot{m}_e = \rho_e A_e v_5 \tag{5}$$

where A_e denotes the nozzle exit area. In the present study, the nozzle exit diameter was 37 mm, and the exit area was determined from

$$A_e = \frac{\pi D^2}{4} \tag{6}$$

The mass emission rate of each exhaust species was calculated from the measured concentration and exhaust mass flow rate as

$$Q_i = X_i \dot{m}e \frac{MW_i}{MW\,\mathrm{mix}} \tag{7}$$

where Q_i is the mass emission rate of species i, X_i is the measured volumetric concentration, MW_i is the molecular weight of the target species, and MW_{mix} is the mean molecular weight of the exhaust gas mixture. The calculated emission rates were subsequently used as source terms in the atmospheric dispersion analysis. The atmospheric concentration of each exhaust species was estimated using the Gaussian plume model,

$$C(x,y,z) = \frac{Q_i}{2\pi U \sigma_y \sigma_z} \exp\left(-\frac{y^2}{2\sigma_y^2}\right)\left[\exp\left(-\frac{(z-H)^2}{2\sigma_z^2}\right) + \exp\left(-\frac{(z+H)^2}{2\sigma_z^2}\right)\right] \tag{8}$$

where C is the atmospheric concentration, U is the ambient wind speed, H is the effective release height, and σ_y and σ_z are the horizontal and vertical dispersion coefficients. Atmospheric stability

was assumed to correspond to neutral conditions (Pasquill–Gifford stability class D), wind speed was set to 1.0 m/s, and exhaust release height was set to 0.5 m. The concentrations were evaluated at a downwind distance of 10 m along the plume centerline ($x = 10$ m, $y = 0$ m, $z = 0$ m).

Figure 7 shows the predicted atmospheric concentrations of CO, CO_2, and NO at a downwind distance of 10 m as functions of the engine rotational speed and biofuel blend ratio. The CO concentration ranged from approximately 183 to 239 mg/m^3 and exhibited a non-monotonic dependence on both the engine rotational speed and the biofuel blend ratio. At low blend ratios, the minimum CO concentration was observed in the rotational speed range of approximately 90,000–95,000 rpm, whereas higher blend ratios generally resulted in increased CO concentrations, particularly at a blend ratio of 50%. Because CO is a typical product of incomplete combustion, the increase in CO concentration observed at high blend ratios is likely attributable to changes in the atomization and evaporation characteristics of the blended fuel. The increase in viscosity and decrease in volatility associated with higher biofuel content may have deteriorated fuel–air mixing, thereby causing locally fuel-rich regions and incomplete oxidation of CO.

The CO_2 concentration ranged from approximately 3,730 to 5,760 mg/m^3 and increased monotonically with engine rotational speed for all blend ratios. In contrast to CO, the influence of the blend ratio on the CO_2 concentration was comparatively small. This behavior suggests that CO_2 formation was governed primarily by the fuel consumption rate and total heat release rather than the fuel composition. As the engine rotational speed increased, the fuel mass flow rate and combustion intensity increased, promoting more complete carbon oxidation and consequently yielding higher CO_2 concentrations.

The NO concentration ranged from approximately 0.32 to 0.89 mg/m^3. For all the blend ratios, the NO concentration increased with the engine rotational speed, whereas increasing the biofuel blend ratio substantially reduced the NO concentration. At 100,000 rpm, the NO concentration decreased from 0.802mg/m^3 for neat conventional fuel to 0.517mg/m^3 at a blend ratio of 50%, corresponding to a reduction of approximately 36%. Because thermal NO formation is strongly dependent on flame temperature via the extended Zeldovich mechanism, this result suggests that increasing the biofuel blend ratio reduced the adiabatic flame temperature and/or the spatial extent of high-temperature reaction zones within the combustor, thereby suppressing thermal NO formation.

Overall, the atmospheric dispersion analysis revealed distinct formation and dispersion characteristics for each exhaust species investigated in this study. The CO_2 concentration was governed mainly by the engine rotational speed and fuel consumption rate, whereas the NO concentration was strongly influenced by both the engine operating condition and fuel blend ratio. Among the investigated species, NO exhibited the most pronounced reduction with increasing biofuel content, indicating the potential of biofuel blending to mitigate nitrogen oxide emissions from small-gas-turbine engines. However, the increase in CO concentration observed at high blend ratios suggests that the combustion efficiency may deteriorate under certain operating conditions. Therefore, further improvements in fuel atomization, evaporation characteristics, and combustor design are required to simultaneously suppress NO emissions while maintaining low levels of CO. These results demonstrate that biofuel blending can effectively modify the atmospheric concentration distribution of exhaust species and is a promising approach for improving the environmental performance of small gas turbine engines.

5. Conclusion

This study evaluated the engine performance, exhaust emission characteristics, LTO-cycle emissions, and atmospheric environmental impact of coconut oil-derived biofuel blends in a small gas turbine engine. The biofuel was synthesized from coconut oil using a low-energy co-solvent transesterification method with ethanol and acetone as co-solvents. The produced fuel was primarily composed of medium-chain fatty acid ethyl esters, particularly ethyl octanoate and ethyl decanoate, with a purity of 97.66%. Combustion experiments were conducted using a small turbojet engine with biofuel blend ratios ranging from 10% to 50%, and the following conclusions were obtained.

First, the combustion efficiency depended on both the biofuel blend ratio and the engine rotational speed. B20 and B30 maintained relatively high combustion efficiencies comparable to that of neat

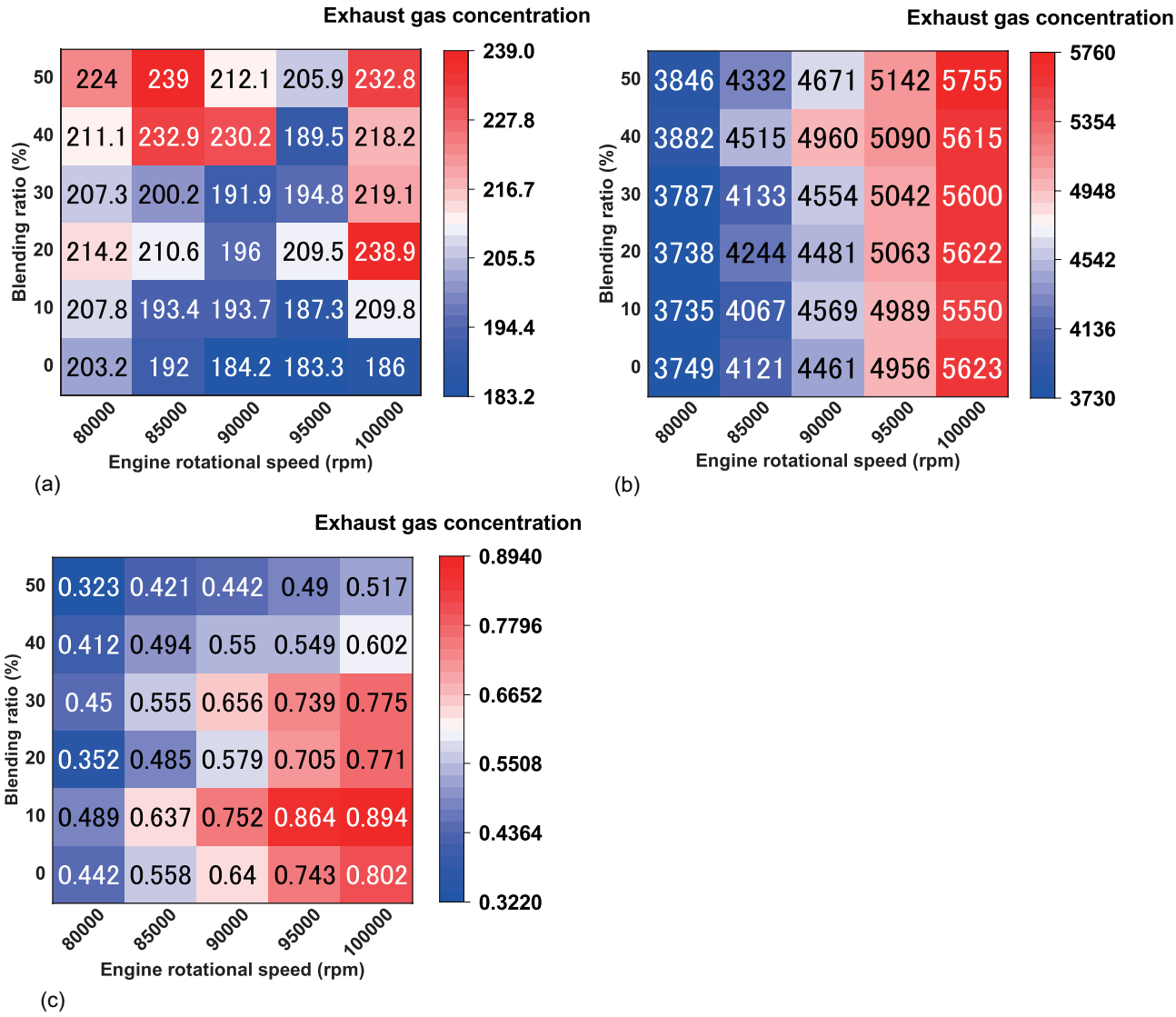


Figure 7 – Predicted atmospheric concentrations of (a) CO, (b) CO_2, and (c) NO at a downwind distance of 10 m as functions of engine rotational speed and biofuel blend ratio.

conventional jet fuel. In particular, B20 exhibited stable combustion characteristics over a wide rotational speed range, whereas B30 exhibited the lowest specific fuel consumption among all fuel conditions. These results indicate that biofuel blend ratios of approximately 20–30% provide a favorable balance between combustion stability and fuel economy under the present experimental conditions.
Second, the emission indices of CO_2 and NO generally decreased with increasing biofuel blend ratio, particularly under high rotational speed conditions. At 100,000 rpm, the reductions in $EICO_2$ and EINO became more pronounced from B20 onward, and the lowest values were observed at B50. This tendency suggests that increasing the biofuel content can suppress CO_2 and NO emissions by modifying fuel composition and combustion temperature. In contrast, the emission index of CO did not vary monotonically with the blend ratio, indicating that the combustion completeness was strongly affected by changes in the spray atomization, evaporation, and fuel–air mixing characteristics.
Third, the LTO-cycle-based emission analysis showed that the taxi/idle phase made the largest contribution to the total CO_2 and NO emissions for all fuel conditions. This was primarily due to the long operating duration of the taxi/idle phase, despite the low thrust setting. B20 and B50 reduced the total NO emissions compared with neat conventional fuel, demonstrating the potential of coconut-oil-derived biofuel blends to mitigate airport-related emissions during representative aircraft operating modes.
Finally, atmospheric dispersion analysis using a Gaussian plume model revealed that the predicted near-field concentrations of exhaust species were strongly dependent on both the engine operating

conditions and biofuel blend ratio. The CO_2 concentration was governed mainly by the engine rotational speed and fuel consumption rate, whereas NO concentration showed a clear reduction with increasing biofuel content. At 100,000 rpm, the predicted NO concentration at 10 m downstream decreased from 0.802 mg/m^3 for neat conventional fuel to 0.517 mg/m^3 for B50, corresponding to a reduction of approximately 36%. These results demonstrate that coconut oil-derived biofuel blending can reduce NO emissions and modify the atmospheric concentration distribution of exhaust species. Overall, coconut-oil-derived biofuel blends produced via a low-energy co-solvent method showed promising applicability as blending components for small-gas-turbine engines. The results indicate that moderate blend ratios, particularly B20–B30, are effective for maintaining combustion performance and reducing specific fuel consumption, whereas higher blend ratios, such as B40–B50, are effective for reducing CO_2 and NO emissions. However, the increase in CO emissions observed under certain conditions indicates that further optimization of fuel atomization, evaporation characteristics, and combustor operating conditions is necessary to simultaneously achieve low NO emissions and complete combustion of the fuel.

Acknowledgements

This work was supported by an Osaka City Innovation Support Grant and research grant of 2025 from Amano Institute of Technology.

Contact Author Email Address

mailto: shinichiro.ogawa@omu.ac.jp

Copyright Statement

The authors confirm that they, and/or their company or organization, hold copyright on all of the original material included in this paper. The authors also confirm that they have obtained permission, from the copyright holder of any third party material included in this paper, to publish it as part of their paper. The authors confirm that they give permission, or have obtained permission from the copyright holder of this paper, for the publication and distribution of this paper as part of the ICAS proceedings or as individual off-prints from the proceedings.

References

[1] Md Fahim Shahriar and Aaditya Khanal. The current techno-economic, environmental, policy status and perspectives of sustainable aviation fuel (saf). *Fuel*, 325:124905, 2022.

[2] Lina Martinez-Valencia, Manuel Garcia-Perez, and Michael P. Wolcott. Supply chain configuration of sustainable aviation fuel: Review, challenges, and pathways for including environmental and social benefits. *Renewable and Sustainable Energy Reviews*, 152:111680, 2021.

[3] ICAO. *CORSIA Methodology for Calculating Actual Life Cycle Emissions Values*. ICAO, 2025.

[4] Tim Edwards. Liquid fuels and propellants for aerospace propulsion: 1903-2003. *Journal of Propulsion and Power*, 19(6):1089–1107, 2003.

[5] Shinichiro Ogawa, Takayuki Matsushita, Takuto Hongo, Yasuaki Maeda, Huynh Phuong Uyen Nguyen, and Koichi Mori. Improving combustion characteristics of fatty acid esters derived from coconut oil for aviation biofuel applications. *Proceedings of AIAA AVIATION FORUM AND ASCEND 2025*, AIAA Paper 2025-3259, 2025.

[6] ASTM International. Standard specification for aviation turbine fuel containing synthesized hydrocarbons. Technical Report ASTM D7566-21, ASTM International, 2022.

[7] Yasuaki Maeda, Le Tu Thanh, Kiyoshi Imamura, Katsutoshi Izutani, Kenji Okitsu, Luu Van Boi, Pham Ngoc Lan, Nguyen Cong Tuan, Young Eok Yoo, and Norimichi Takenaka. New technology for the production of biodiesel fuel. *Green Chem.*, 13:1124–1128, 2011.

[8] Miaojia Song, Xinghua Zhang, Yubao Chen, Qi Zhang, Lungang Chen, Jianguo Liu, and Longlong Ma. Hydroprocessing of lipids: An effective production process for sustainable aviation fuel. *Energy*, 283:129107, 2023.

[9] Konstantinos Atsonios, Jun Li, and Vassilis J. Inglezakis. Process analysis and comparative assessment of advanced thermochemical pathways for e-kerosene production. *Energy*, 278:127868, 2023.

[10] Hitoshi Fujiwara, Masaharu Nakamura, Ryouma Hiyamizu, Hideshi Yamada, Kazuo Shimodaira, Masashi Hirota, and Keiichi Okai. Engine test of small gas turbines with aviation bio jet fuel. *Journal of the Gas Turbine Society of Japan*, 44:182–188, 2016.

[11] Zehra Habib, Ramkumar Parthasarathy, and Subramanyam Gollahalli. Performance and emission characteristics of biofuel in a small-scale gas turbine engine. *Applied Energy*, 87(5):1701–1709, 2010.

[12] Murat Kadir Yesilyurt, Tanzer Eryilmaz, and Mevlüt Arslan. A comparative analysis of the engine performance, exhaust emissions and combustion behaviors of a compression ignition engine fuelled with biodiesel/diesel/1-butanol (c4 alcohol) and biodiesel/diesel/n-pentanol (c5 alcohol) fuel blends. *Energy*, 165:1332–1351, 2018.

[13] Misel J Sisi, M Rafiuddin Ahmed, and David Rohindra. Performance and emission characteristics of a diesel engine employing straight vegetable oils from vanuatu as fuels. *Advances in Mechanical Engineering*, 12(9):1687814020962351, 2020.

[14] Hanh Ngoc Thi Le, Kiyoshi Imamura, Norie Watanabe, Masakazu Furuta, Norimichi Takenaka, Luu Van Boi, and Yasuaki Maeda. Biodiesel production from rubber seed oil by transesterification using a co-solvent of fatty acid methyl esters. *Chemical Engineering & Technology*, 41(5):1013–1018, 2018.

[15] Thao Pham Thi Phuong, Uyen Nguyen Huynh Phuong, Kiyoshi Imamura, Masakazu Furuta, and Yasuaki Maeda. Transesterification using isopropanol as a co-solvent for the production of green biodiesel fuel. *International Journal of Energy Research*, 46(4):4352–4361, 2022.

[16] Shinichiro Ogawa, Koichi Mori, and Yasuaki Maeda. Study on combustion characteristics of coconut saf using micro jet engine. *International Journal of Gas Turbine, Propulsion and Power Systems*, 15(5):v15n5tp06, 2024.

[17] Takuto Hongo, Shinichiro Ogawa, Koichi Mori, Yasuaki Maeda, and Huynh Phuong Uyen Nguyen. Verification of the combustion characteristics and exhaust gas components of fatty acid ethyl esters derived from coconut oil using a small jet engine. *JOURNAL OF THE JAPAN SOCIETY FOR AERONAUTICAL AND SPACE SCIENCES*, 73(1):1–9, 2025.

[18] Shinichiro Ogawa, Takuto Hongo, Yasuaki Maeda, Huynh Phuong Uyen Nguyen, and Koichi Mori. Combustion and emission characteristics of aviation biofuel derived from coconut oil using the co-solvent method: toward eco-friendly micro jet engines. *Fuel*, 428:140208, 2027.

[19] Ramraj H. Sundararaj, Roshan Dinesh Kumar, Anoop Kumar Raut, T. Chandra Sekar, Vivek Pandey, Abhijit Kushari, and S.K. Puri. Combustion and emission characteristics from biojet fuel blends in a gas turbine combustor. *Energy*, 182:689–705, 2019.

[20] T. Suchocki, L. Witanowski, P. Lampart, P. Kazimierski, K. Januszewicz, and B. Gawron. Experimental investigation of performance and emission characteristics of a miniature gas turbine supplied by blends of kerosene and waste tyre pyrolysis oil. *Energy*, 215:119125, 2021.

[21] IPCC. Good practice guidance and uncertainty management in national greenhouse gas inventories. Technical report, 2000.

[22] D. M. M. S. Dissanayaka, V. V. Adikariwattage, and H. R. Pasindu. Evaluation of co2 emission at airports from aircraft operations within the landing and take-off cycle. *Transportation Research Record*, 2674(6):444–456, 2020.

[23] Junli Yang, Likun Li, Xiaoyu Zheng, Hang Liu, Fengming Li, and Yi Xiao. Pollutant dispersion of aircraft exhaust gas during the landing and takeoff cycle with improved gaussian diffusion model. *Atmosphere*, 15(10), 2024.